Miniaturised Electrochemical Analyser for Glucose Determination Based on Chitosan/GOD/Electroreduced Graphene Oxide Sensor

Zemin Zhang[1,2], Huihuang Wu[1,2], Yueming Gao[1,2,*], Linke Huang[1,2], Haibo Pan[2], Ming Du[1,3]

[1] College of Physics and Information Engineering, Fuzhou University, Fuzhou 350116, China
[2] Key Lab of Medical Instrumentation & Pharmaceutical Technology of Fujian Province, Fuzhou 350116, China
[3] Key Lab of Eco-Industrial Green Technology of Fujian Province, Wuyi University, Nanping 354300, China.
[*]E-mail: fzugym@gmail.com

This paper aimed to design a miniaturised electrochemical analyser (MEA) for glucose determination based on the integration of chitosan (CS), glucose oxidase (GOD) and electroreduced graphene oxide (e-RGO). The low-power programmable analog front-end LMP91000 and the microcontroller STM32F103C8T6 were combined into the hardware system of the MEA. The potentiostat function of the system was realised by applying the setting potential on the three-electrode sensor. By setting the trans-impedance gain, the current can be converted from a full range of 5 μA to 750 μA. The voltage signal was converted into the current signal using an algorithm to process the experimental results. Reliability of the MEA was verified by electrochemical workstation, and the performance was tested using a $[Fe(CN_6)]^{3-}$ solution. The MEA showed a good linear relationship between the final steady-state current and the $[Fe(CN_6)]^{3-}$ concentration in the dynamic range of 0.2 mM to 10 mM (R^2= 0.9841). GOD was fixed on a working electrode (WE) modified with e-RGO to prepare the glucose sensor. Finally, different glucose concentrations were measured using chronoamperometry with the MEA. The MEA sensitivity reached 169.32 mA/M·cm^{-2}, and the limit of detection amounted to 0.19 mM according to 3δ/slope calculation.

1. INTRODUCTION

Portability, automation and intelligence are important development trends in the field of medical testing instruments for current medical needs. Miniaturised portable testing instruments can be

used for early detection of diseases (e.g. diabetes) and personalised health care [1-2]. Electrochemical analysis technology is widely used in miniaturised analytical systems due to its high sensitivity, good repeatability, low limit of detection (LoD) and low cost [3-4]. As a common and current analysis method, chronoamperometry is used to induce the redox reaction of active molecules on the electrode by applying a single or double-potential step to the working electrode (WE) of the electrochemical system [5-7]. The relationship between the current response and time is detected during the reaction.

The existing electrochemical equipment in the laboratory includes CHI600E and CHI660D of CHI series and PGSTAT204 electrochemical workstation of Autolab series. Its large size and need for specialised training make this equipment unsuitable for use outside the laboratory. The miniaturised electrochemical detection system can directly interact with the biological samples to be detected; hence, the required information such as physiological variables can be obtained quickly and conveniently [8]. Therefore, the development of miniaturised, portable and intelligent electrochemical detection equipment is important for real-time detection in the medical field [9].

Xing et al. proposed a low-cost wearable electrochemical glucose sensor. The glucose sensor was prepared by modifying chitosan–GOD on the WE surface [10]. Curto et al. proposed an autonomous wearable microfluidic system for real-time pH analysis of sweat [11]. Somayeh et al. designed a wearable hybrid sensor system. A three-electrode lactic acid biosensor and a two-electrode electrocardiogram sensor were designed on the same flexible substrate, which allowed real-time monitoring of biochemical (lactic acid) and electrophysiological signals (electrocardiogram) [2]. Chaiyo et al. proposed non-enzyme detection of glucose using cobalt phthalocyanine, graphene and ionic liquid, which modified the screen-printed carbon electrode. The modified carbon electrode exhibited excellent electrocatalytic activity for glucose with NaOH as the supporting electrolyte [12]. Sohini et al. designed an enzyme biosensor that could be used to detect uric acid in wound fluid. The sensor of the electrochemical detection device contains uric acid oxidase, which can detect uric acid in wound fluid continuously for one week at normal temperature [13]. Daizong et al. designed a miniaturised detection system based on a smart phone. The system consists of a graphene-modified screen-printed electrode, an electrochemical detection device and a smart phone that can be used for cyclic voltammetry detection [14]. Chronoamperometry features a higher sensitivity, faster detection time and is more suitable for real-time detection compared with cyclic voltammetry. A graphene-modified WE can improve the electron transfer rate of sensors and shorten detection time.

In the present work, we designed a chronoamperometry-capable miniaturised electrochemical analyser (MEA) based on electroreduced graphene oxide (e-RGO). The device consists of two parts: a three-electrode sensor and an embedded system. The embedded system consists of an analog front-end based on LMP91000 (LMP) chip and a microcontroller STM32F103C8T6 (STM32), which is mainly used to control the measurement mode of sensors and to display, store and process experimental results. $[Fe(CN)6]^{3-}$ was used as redox couple to determine the sensitivity and LoD of the MEA; it was also used to verify the repeatability and accuracy of the proposed analyser. The glucose sensor was prepared by dropping GOD onto the surface of the electrode modified with e-RGO. The chronoamperometric response of the glucose sensor at different glucose concentrations was measured by the MEA.

The rest of our paper is organised as follows: Section 2 discusses the design and development

of the MEA and its system verification. The WE was modified with e-RGO to improve the sensor performance. Chronoamperometric detection of glucose at different concentrations was performed using the improved sensor. Section 3 presents the experimental results and phenomenon in the experiment. Lastly, Section 4 presents the conclusions of this paper.

2. MATERIALS AND METHODS

2.1. Design and development of the MEA

The programmable analog front-end LMP and the microcontroller STM32 were used to design the MEA. The LMP chip with an average voltage of 3.3 V and a total current consumption of 10 µA was selected to meet the requirements of miniaturisation, low cost and low power. LMP provides a complete signal path for the connection between the sensor and the microcontroller. LMP was powered and controlled by the microcontroller via its I^2C interface. STM32 controls LMP to realise the function of potentiostat. It applies the excitation signal (relative to the reference electrode (RE)) to the WE accurately, drives the solution to react, and generates stable current in the current circuit composed of the working electrode and the counter electrode (CE). Figure 1 shows the flow chart of the whole experiment.
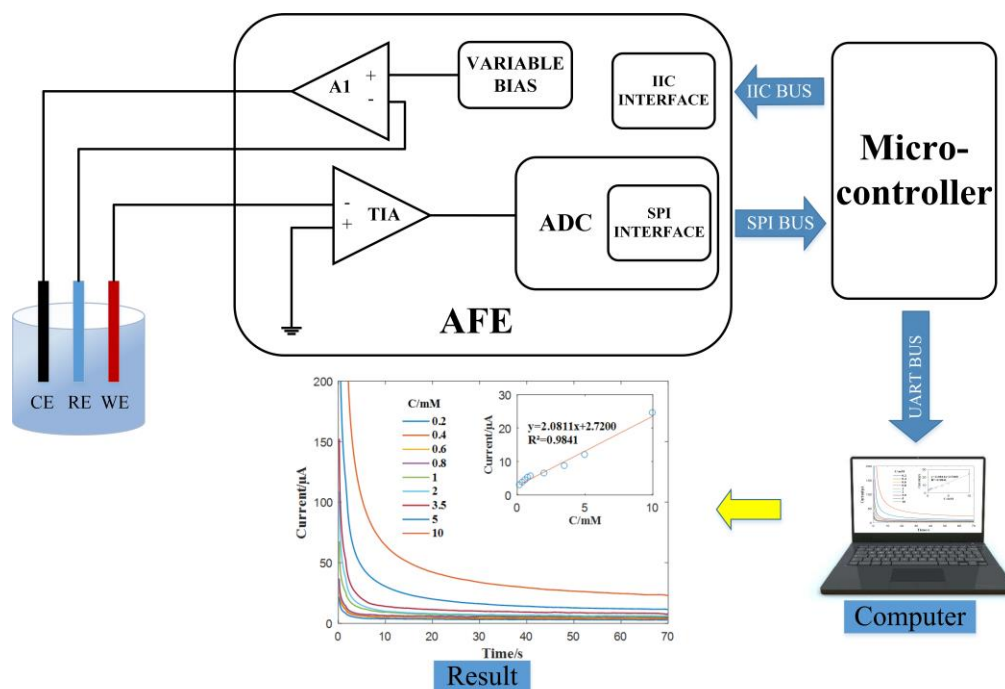

Figure 1. Electrochemical response diagram of the glucose detection device base on a miniaturised electrochemical analyser (MEA).

Using Keil 5 to program the BIAS register of LMP, the potential of WE versus RE can be set in the range of ± 0.6 V. The TIACN register configures the resistance value of the trans-impedance

amplifier and that between the trans-impedance amplifier and the WE. The current conversion from a full range of 5 µA to 750 µA was realised by setting the trans-impedance gain, which can achieve the low-concentration electrochemical detection. The analog front-end converts the analogue voltage signal into digital voltage through the analogue-to-digital converter (ADC, ADC161S626, TI). The sampling rate of ADC was programmed through Keil 5, and the sampled data were transmitted to STM32 via the serial peripheral interface (SPI). The voltage signal was converted into the current signal through the algorithm in STM32, and the data were preliminarily analysed. Formula 1 shows the relationship between these settings. Figure 2 displays the software control flow chart. During the entire experiment, the analogue voltage was digitised by automatic measurement of the MEA. Moreover, the current time data were recorded and then transmitted to the computer through the microcontroller. The experimental data were processed and plotted in MATLAB.
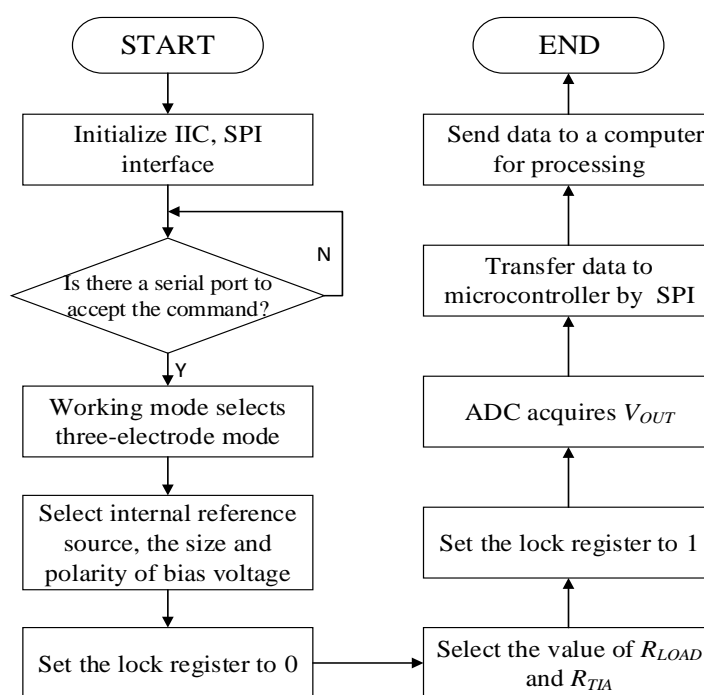
Figure 2. Software program flow chart.

$$I_{out} = (V_{out} - V_{INT\_Z}) / TIA_{gain} \tag{1}$$

2.2 $[Fe(CN_6)]^{3-}$ reduction

$[Fe(CN_6)]^{3-}$ solutions with different concentrations (c=0.2, 0.4, 0.6, 0.8, 1, 2, 3.5, 5, 10 mM) were prepared (potassium ferricyanide:potassium ferrocyanide:potassium chloride = 1:1:1). Potassium ferricyanide, potassium ferrocyanide and potassium chloride were purchased from Sinopharm Chemical Reagent Co., Ltd (Shanghai, China). A 3 mm glassy carbon electrode (GCE), platinum electrode and Ag/AgCl electrode were used as WE, CE, and RE, respectively. The WE was first polished with Al_2O_3 powders of different particle sizes (0.3 µm and 0.05 µm) and ultrasonically

washed with deionised water and ethanol. Finally, the surface of the WE was dried with nitrogen. The reduction potential of the WE was set as –0.6 V versus the RE. The experimental data were recorded by programming at a time interval of 0.1 s and transmitted to the upper computer software for storage in real-time. A total of 70 s of experimental data were recorded. All the experimental data were smoothed in MATLAB using a moving average filter. The final steady-current of each concentration of the $[Fe(CN_6)]^{3-}$ solution was calculated as the average value of 30 data points around t=60 s. The experiment was repeated independently on an electrochemical workstation as a comparative trial.

2.3 Fabrication of e-RGO/GCE with improved sensor performance

Graphene oxide (GO) was purchased from Nanjing Xianfeng Nano Materials Technology Co., Ltd (Nanjing, China). The aqueous dispersion of GO was physically exfoliated by sonication to reduce the van der Waals force between the two-dimensional layers of GO [15]. The exfoliated GO (5 μL, 2 mg/mL) was dropped onto the bare GCE and placed in a laboratory oven at 60 ℃ for 20 min. After cooling for several minutes, the GO/GCE was electroreduced using the electrochemical workstation CHI 660D. Ten cyclic voltammetric scans (potential range –1.5 V to 0 V, scanning rate 0.05 v/s) were run in 10 mM PBS buffer to realise the successful deposition of e-RGO on the electrode surface. The electrochemical reactions of bare GCE, GO/GCE and e-RGO/GCE in $[Fe(CN_6)]^{3-}$ solution (50 mL, 1 mM) were measured by the MEA. The currents before and after modification were compared to verify the improved performance of the electrochemical sensor [16].

2.4 Glucose sensing experiments

A total of 0.01 g chitosan (CS) was dissolved in acetic acid solution (1 mL, 8%) to obtain a 1 mL chitosan solution. Afterward, 20 mg/mL GOD solution and 1 mL chitosan solution were mixed at a volume ratio of 2:1. Physical exfoliation was performed by sonication for 10 minutes to obtain the desired GOD-CS solution. 5 μL GOD-CS solution was dropped onto the surface of e-RGO/GCE and dried in an oven at 37 ℃ for 3 h to get the glucose sensor (GOD-CS/e-RGO/GCE). Glucose standard solutions with different concentrations (c=0.05, 0.1, 0.2, 0.3, 0.4, 0.5, 1 mM) were prepared with 100 mM PBS buffer with pH = 7.4. The MEA was used to detect the chronoamperometric response of the glucose sensor at different glucose concentrations.

2.5 Glucose determination in real sample

Artificial sweat was selected as the real sample to evaluate the applicability of GOD-CS/e-RGO/GCE as a glucose sensor. The determination of glucose in the artificial sweat samples was quantitatively analyzed by the MEA. Based on the composition of natural sweat, artificial sweat (for 1 L: NaCl 20 g, NH_4Cl 17.5 g, CH_4N_2O 5 g, CH_3COOH 2.5 g, $C_3H_6O_3$ 15 g, appropriate NaOH) was formulated.

3. RESULTS AND DISCUSSION

3.1 Reliability verification of the device

The chronoamperometric response of $[Fe(CN_6)]^{3-}$ solution (50 mL, 1 mM) was recorded by the MEA and electrochemical workstation under the same experimental conditions (T=25 ℃, t=70 s) to verify reliability and accuracy of the MEA.
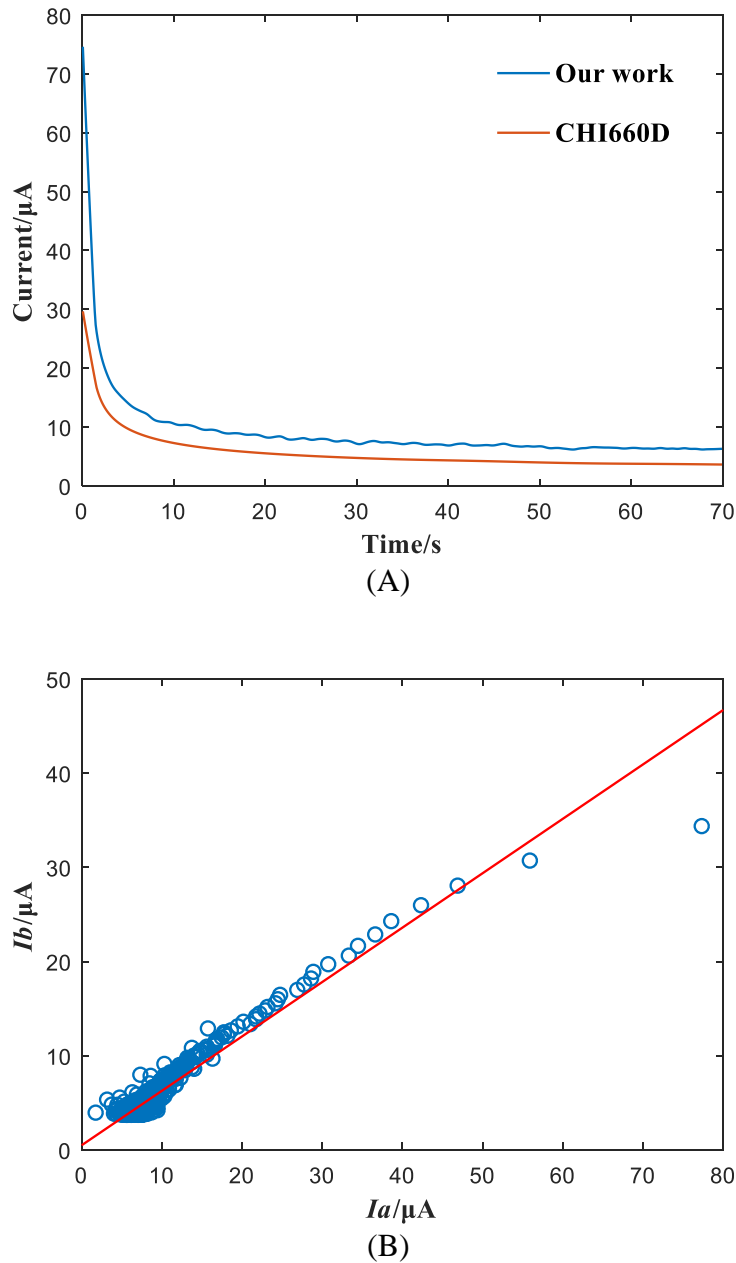

(A)

(B)

Figure 3. (A) Chronoamperometry experimental diagram of the electrochemical workstation and the MEA in 50 mL 1 mM $[Fe(CN_6)]^{3-}$ solution (I-t response); (B) correlation analysis between the two devices ($y = 0.5775x + 0.0005$, $r = 0.9696$), where I_a and I_b are the current response of the MEA and the electrochemical workstation.

Figure 3(A) shows the experimental comparison results. The figure shows that MEA can detect a high current response at the initial time of voltage application. Figure 3(B) shows the correlation analysis diagram of the two devices, with the correlation coefficient $r=0.9696$ ($y=0.5775x+0.0005$). The findings prove the strong correlation between the two devices. Compared with the electrochemical workstation, the experimental results show that the MEA features high reliability and accuracy.

Three different concentrations of $[Fe(CN_6)]^{3-}$ solution (c=1, 5, 10 mM) were detected 10 times at a constant sampling rate (sample/s) under the same experimental conditions. Table 1 shows the current response values at different concentrations. The table indicates that when the solution concentration was 10 mM, the coefficient of variation (CV) reached 2.57%. The CV decreased significantly with the increase in solution concentration. The experimental results show that the MEA exhibits good repeatability in the chronoamperometric experiments with different concentrations.

Table 1. Chronoamperometry repeatability experiment

The final steady-state current	$C/[Fe(CN)_6]^{3-}$		
	1 mM	5 mM	10 mM
The response current (μA)	5.86±0.40	10.71±0.53	24.17±0.62
CV%	6.89	5.02	2.57

3.2 *[Fe(CN₆)]³⁻ reduction*

The $[Fe(CN_6)]^{3-}$ reaction on the WE was a diffusion controlled reduction reaction. The changing process of the chronoamperometric response of the WE in $[Fe(CN_6)]^{3-}$ solution can be expressed using Formula (2). The chronoamperometric response of the $[Fe(CN_6)]^{3-}$ solution with concentrations ranging from 0.2 mM to 10 mM was measured by the MEA. Figure 4 shows the experimental results of the chronoamperometric (current–time) response. Each experiment was conducted under the same experimental conditions. The experiment temperature was maintained at 25 ℃. A reduction potential of –0.6 V versus the RE was applied to the WE. A total of 70 s of experimental data were recorded at a rate of 10 sample/s. The change trend of the curve in Figure 4 was consistent with that of the experimental change curve obtained by the electrochemical workstation in Figure 3(A). The experimental results show that the MEA can detect chronoamperometric response at different concentrations. Figure 4 shows that the current reached stability within the set time (70 s), and the final steady-state current and solution concentration follow the Cottrell equation shown in Formula (3) :

$$[Fe(CN)_6]^{3-}+e^{-}\rightarrow[Fe(CN)_6]^{4-} \qquad (2)$$

$$I(t) = \frac{nFAD^{1/2}c_0}{\pi^{1/2}t^{1/2}} \qquad (3)$$

where I (A) is the final steady-state current; c_0 (mM) is the initial concentration of the solution; A (cm²) is the area of the WE; F is Faraday's constant; D (cm²/s) is the diffusion coefficient; n is the

number of electron transfer; T (s) is time. Formula (3) indicates that the final steady-state current is linear with the initial solution concentration when other conditions remain unchanged. Thus, the final steady-state current can be used as an analytical parameter. From the inset in Figure 4, the curve of the final steady-state current and the $[Fe(CN)_6]^{3-}$ concentration is linear in this concentration range: $y=2.0811x+2.7200$, and $R^2=0.984$, where y (µA) is the reduction current, and x is the concentration of $[Fe(CN)_6]^{3-}$ solution. The sensitivity and LoD with 3δ/slope calculation reached 92.49 mA/M·cm^{-2} and 0.13 mM, respectively.
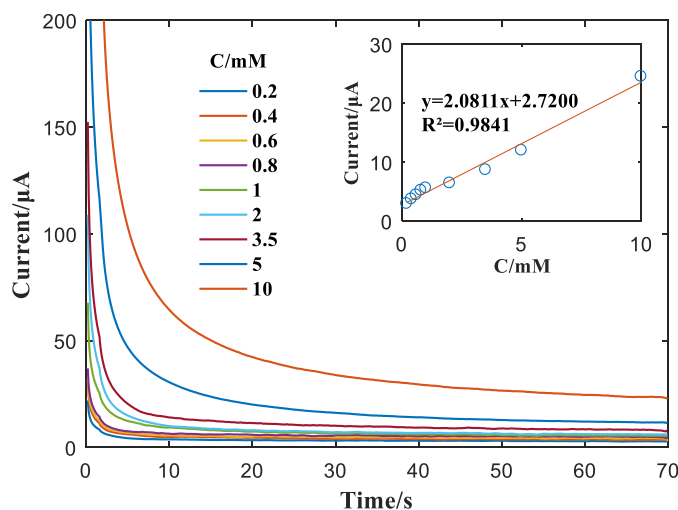

Figure 4. Response diagram of chronoamperometry measured by the MEA in the reduction reaction of $[Fe(CN_6)]^{3-}$ solution. The inset shows the fitted function of the average steady-state current versus the potassium ferricyanide concentration.

3.3 Fabrication of e-RGO/GCE with improved sensor performance

The electrode surface is often modified using nano-materials to improve sensor performance and obtain a functional electrode surface with high selectivity and sensitivity [17]. Compared with other nano-materials, solid graphene presents a larger specific surface area and higher electrocatalytic activity [18]. However, solid graphene undergoes evident agglomeration phenomenon. Therefore, GO with good hydrophilicity was used to modify the electrode surface. The chronoamperometric response of the electrode before and after modification was measured using the MEA in 50 mL PBS buffer (100 mM, pH = 7.4). Figure 5 shows the experimental results. The figure reveals that the current response of the electrode modified with GO was lower than that of the bare GCE. This finding is due to the presence of a large number of oxygen-containing functional groups on GO, which resulted in the decreased conductivity of the modified electrode [19-20]. e-RGO was used to functionalise the WE surface to improve the conductivity of the latter [21]. e-RGO was prepared by electroreduction of GO on the electrochemical workstation using cyclic voltammetry (10 cyclic voltammetric scans, voltage range from –1.5 V to 0 V). The figure shows that when GO was reduced to e-RGO, the response current of the WE was recovered and was significantly greater than that of the bare GCE. Therefore,

sensor sensitivity can be improved using the high-conductivity e-RGO; furthermore, enzymes and other substances can be better adsorbed when the electrode is immobilised with an enzyme [22].
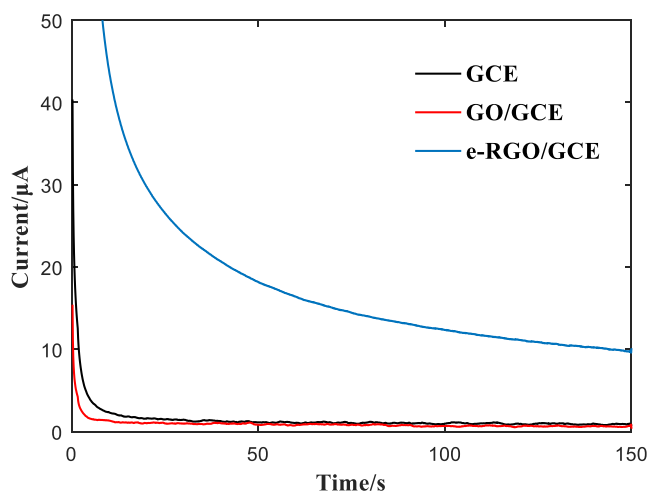

Figure 5. Chronoamperometric response of bare GCE, GO-GCE and e-RGO-GCE in 50 mL 100 mm PBS buffer (pH = 7.4) as measured by the MEA.

3.4 Glucose sensing experiments

Figure 6 shows the response of chronoamperometry obtained by the reaction of glucose at different concentrations with GOD on the sensor. The current–time curve within 150 s was also recorded. It can be observed that the modified electrode showed good electrocatalytic ability .
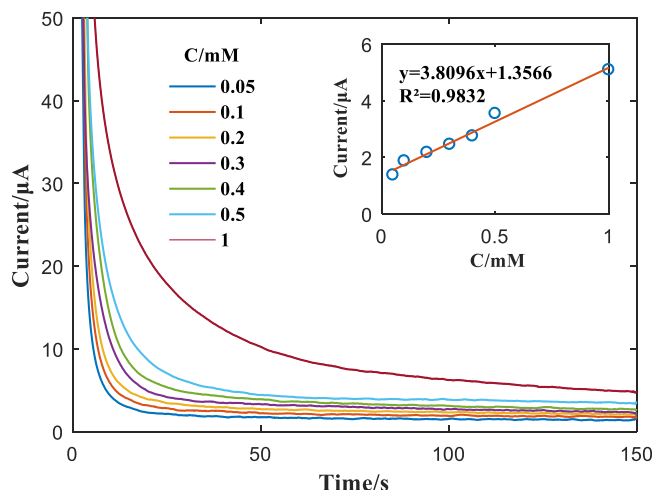

Figure 6. Chronoamperometric response of GOD-e-RGO/GCE with different glucose concentrations (i.e. 0.05 mM to 1 mM) as measured by the MEA. The inset shows the calibration curve of GOD-e-RGO/GCE for glucose solutions of different concentration gradients.

The final steady-current was calculated as the average value of 30 data points between t=135 s and t=140 s. Curve fitting was performed between the final steady-state current and the glucose

solution concentration. The fitting result is shown in the inset of Figure 6 and was computed as follows: $y=3.8096x+1.3566$, $R^2=0.9832$, where y (mM) is the glucose solution concentration, and x is the final steady-state current. Figure 6 shows the good linear relationship between the glucose concentration and final steady-state current in the measurement range. The sensitivity and LoD with 3δ/slope calculation measured 169.32 mA/M·cm^{-2} and 0.19 mM, respectively.

3.5 Glucose determination in real sample

We investigated the applicability of the glucose sensor in artificial sweat as the real sample. Table 2 shows the experimental results obtained by the standard addition method. The analyser could detect the determination of glucose with acceptable recovery and RSD (less than 5.2%). It shows that the coupling of the MEA and GOD-CS/e-RGO/GCE could be used to determine glucose in artificial sweat with good applicability.

Table 2. Determination of glucose in artificial sweat

Sample	Glucose added (mM)	Glucose found (mM)	RSD (%, n=3)	Recovery (%)
1	0.20	0.16	5.2	81.0
2	0.60	0.71	4.7	118.2
3	1.00	1.10	4.0	110.0

4. CONCLUSION

A portable and intelligent MEA was proposed in the present paper. The MEA was designed with the analog front-end and STM32. The low-power LMP chip can provide a reliable transmission scheme between the three-electrode sensor and the microcontroller. The analog voltage signal obtained by the sensor was converted into a digital signal by programming the ADC through STM32. The obtained digital voltage signal was transmitted to STM32 via the SPI. The voltage signal was subsequently converted into current signal through the algorithm to conduct preliminary analysis of experimental data. Experimental results of the preliminary analysis were transferred to the upper computer software for data preservation. Finally, the experimental data were processed through programming, and the experimental results were analysed.

Chronoamperometric experiments were performed using the MEA and the electrochemical workstation under the same experimental conditions. The correlation coefficient r of the two devices reached 0.9696 ($y = 0.5775x + 0.0005$), which verified the reliability and accuracy of the detection device. In the performance verification of the device, the final steady-state current of the MEA exhibited a good linear relationship with the $[Fe(CN_6)]^{3-}$ concentration within the wide dynamic range

of 0.2 mM to 10 mM (R^2=0.9841). When the solution concentration was 10 mM, the CV reached 2.57%, and the repeatability of the MEA was within the acceptable range. When the surface of the GCE was modified with e-RGO, the electrode conductivity was substantially improved. The e-RGO/GCE modified by GOD-CS solution showed good sensitivity for glucose detection. The experimental results show the linear relationship between the final steady-state current and glucose concentration (R^2 = 0.9832). The sensitivity of the MEA was 169.32 mA/M·cm^{-2}, and the LoD was 0.19 mM with 3δ/slope calculation. Moreover, GOD-CS/e-RGO/GCE showed good quantitative analysis results of glucose in artificial sweat samples, and its applicability is proved. Future works should focus on further improving the sensitivity of the MEA, reducing its LoD and improving the selectivity of glucose sensor in field detection.

References

1. W. Gao, S. Emaminejad, H. Y. Y. Nyein, S. Challa, K. Chen, A. Peck, H. M. Fahad, H. Ota, H. Shiraki, D. Kiriya, D. Lien, G. A. Brooks, R. W. Davis, A. Javey, *Nature*, 529 (2016) 509.
2. S. Imani, A. J. Bandodkar, A. M. V. Mohan, R. Kumar, S. Yu, *Nature Communications*, 7 (2016) 11650.
3. R. Pruna, F. Palacio, A. Baraket, N. Zine, A. Streklas, J. Bausells, A. Errachid, M. Lópeza, *Biosens. Bioelectron.,* 100 (2018) 533.
4. P. S. Pakchin, S. A. Nakhjavani, R. Saber, H. Ghanbari, Y. Omidi, *Trac-Trend. Anal. Chem.*, 92 (2017) 32.
5. T. C. Canevari, M. Nakamura, F. H. Cincotto, F. M. de Melo, H. Toma, *Electrochim. Acta.*, 209 (2016) 464.
6. L. C. Juanarena, C. Borsjea, T. Sleutels, D. Yntema, C. Santoro, I. Ieropoulos, F. Soavi, A. Heijnea, *Biotechnol. Adv.*, (2019)107456.
7. C. E. Turick, S. Shimpalee, P. Satjaritanun, J. Weidner, S. Greenway, *Appl. Microbiol. biot.*, (2019) 1.
8. A. F. D. Cruz, N. Norena, A. Kaushik, S. Bhansali, *Biosens. Bioelectron.*, 62 (2014) 249.
9. A. Ainla, M. P. Mousavi, M. N. Tsaloglou, J. Redston, J. G. Bell, M. T. F. Abedul, G. M. Whitesides, *Anal. chem.*, 90 (2018) 6240.
10. X. Xuan, H. S. Yoon, J. Y. Park, *Biosens. Bioelectron.*, 109 (2018) 75.
11. V. F. Curto, S. Coyle, R. Byrne, N. Angelov, D. Diamond, F. B. Lopez, *Sensors. Actuat B-Chem.*, 175 (2012) 263.
12. S. Chaiyo, E. Mehmeti, W. Siangproh, T. L. Hoang, H. P. Nguyen, O. Chailapakul, K. Kalcher, *Biosens. Bioelectron.*, 102 (2018) 113.
13. S. Roy, Y. Umasa, J. Jaller, I. Hersk, J. Mervis, E. Darwin, P. A. Hirt, L. J. Borda, H. A. L. Tov, R. Kirsner and S. Bhansali, *J. Electrochem. Soc.*, 165 (2018) B3168.
14. D. Ji, L. Liu, S. Li, C. Chen, Y. Lu, J. Wu, Q. Liu, *Biosens. Bioelectron.*, 98 (2017) 449.
15. I. K. Moon, J. I. Kim, H. Lee, K. Hur, W. C. Kim, H. Lee, *Scientific reports*, 3 (2013) 1112.
16. D. Wang, Y. Liang, Y. Su, Q. Shang, C. Zhang, *Biosens. Bioelectron.*, 130 (2019) 55.
17. A. Baranwal, A. Kumar, A. Priyad, G. S. Oggu, I. Bhatnagar, A. Srivastava, P. Chandra, *Int. J. Biol. Macromol.*, 110 (2018) 110.
18. L. A. Mercante, M. H. Facure, R. C. Sanfelice, F. L. Migliorini, L. H. Mattoso, D. S. Correa,

Appl. Surf. Sci., 407 (2017) 162.
19. K. Krish, M. Veera, K. Yun, S. J. Kim, *Carbon*. 53 (2013) 38.
20. S. M. Li, S. Y. Yang, Y. S. Wang, H. P. Tsai, H. W. Tien, S. T. Hsiao, W. H. Liao, C. L. Chang, *J. Power Sources*, 278 (2015) 218.
21. B. Liang, L. Fang, G. Yang, Y. Hu, X. Guo, X. Ye, *Biosens. Bioelectron.*, 43 (2013) 131.
22. P. Y. Sedeño, S. Campuzano , J. M. Pingarrón, *Anal. Chim. Acta.*, 960 (2017) 1.